

# Monolayer-Protected Cluster Growth Dynamics

Shaowei Chen,<sup>†</sup> Allen C. Templeton, and Royce W. Murray\*

Kenan Laboratories of Chemistry, University of North Carolina,  
Chapel Hill, North Carolina 27599-3290

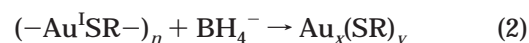
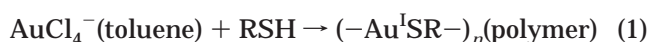
Received September 13, 1999. In Final Form: December 31, 1999

With the objective of better understanding the Brust synthesis reaction, this paper examines the evolution of the core sizes of hexanethiolate monolayer-protected Au clusters (MPCs) in a typical synthesis reaction mixture, at time intervals over the course of 125 h. Transmission electron microscopy shows that the average MPC core diameter gradually increases over the first 60 h of reaction and then remains largely unchanged afterward at  $\sim 3.0$  nm. Differential pulse voltammetry of purified MPC aliquots removed from the synthesis reaction exhibit quantized double-layer (QDL) charging peaks. QDL charging peaks have been previously shown to be a strong function of MPC core size and dispersity and reveal (i) the presence of several discernible core sizes in each sample and (ii) an increase in cluster capacitance ( $C_{\text{CLU}}$ ) with longer reaction times, consistent with the electron microscopy results.

## Introduction

Nanometer-sized metallic and semiconducting particles are an active research area today for a variety of reasons, including generating and understanding materials at the bulk/molecular interface that display interesting size-dependent optical, electronic, and physical properties.<sup>1</sup> keystones to research on nanoparticles are synthetic routes to produce them in a size-controllable manner. A facile synthesis of nanoparticles composed of gold clusters coated with thiolate monolayers (or monolayer-protected gold clusters, Au MPCs), introduced by Schiffrin and co-workers,<sup>2</sup> has attracted extensive use. Au MPCs additionally exhibit stability in both solution and dry forms, allowing characterization using standard analytical approaches<sup>3</sup> and, most importantly from the chemist's perspective, facilitating simple chemical transformations to introduce a wide variety of structural groups<sup>4</sup> onto the nanoparticles.

The MPC synthesis reaction is a two-step process that leads to modestly polydisperse (in core size) alkanethiolate-protected Au clusters with average core diameters of 1.1–5.2 nm.<sup>3,5</sup>



For example, employing hexanethiol as RSH in a 3:1 thiol/Au reactant ratio and chilling the reaction yields a solution of clusters with an average core diameter of 1.6 nm and average  $\text{Au}_{145}(\text{S}(\text{CH}_2)_5\text{CH}_3)_{50}$  composition.<sup>3</sup> The behavior of reactions (1) and (2) is consistent with a nucleation–growth–passivation process; namely, larger thiol/gold mole ratios and fast addition of reductant produce smaller average MPC core sizes,<sup>3,5</sup> and quenching the reaction at short times produces higher proportions of MPCs with very small core sizes ( $< 2$  nm).<sup>6</sup>

Besides these few significant observations, the details of the MPC synthesis reaction remain largely unexplored. In this paper, we address an important unexplored aspect of the synthetic reaction, namely, the phenomenon of slow changes in cluster core size that follow the active earliest stages of the synthetic reaction. An appreciation of the cluster growth mechanism and annealing effects may be useful in designing improved tactics to produce more monodisperse and larger quantities of very small ( $< 1.5$  nm diameter) MPCs. The successful procurement of these materials is, of course, critical to examining important size-dependent core properties free of averaging over a mixed population of different MPC core sizes. For alkanethiolate-protected MPCs, the most interesting core attributes observed thus far are the onset of electrochemical and spectroscopic band gaps below about 100 atoms/core and quantized double-layer (QDL) capacitance charging of the MPC cores in room-temperature electrolyte solutions.<sup>7</sup>

In the experiments described, we follow the core size and dispersity of the hexanethiolate-coated MPC materials produced over a 125 h course of reaction time, using the standard core size measurement method of transmission

\* To whom all correspondence should be addressed. E-mail: rwm@email.unc.edu.

<sup>†</sup> Present address: Department of Chemistry and Biochemistry, Southern Illinois University, Carbondale, IL 62901-4409.

(1) (a) Schmid, G., Ed. *Clusters and Colloids*; VCH: Weinheim, Germany, 1994. (b) Hayat, M. A., Ed. *Colloidal Gold: Principles, Methods, and Applications*; Academic Press: New York, 1989; Vols. 1 and 2. (c) Haberland, H., Ed. *Clusters of Atoms and Molecules*; Springer-Verlag: New York, 1994.

(2) (a) Brust, M.; Walker, M.; Bethell, D.; Schiffrin, D. J.; Whyman, R. *J. Chem. Soc., Chem. Commun.* **1994**, 801–802. (b) Brust, M.; Fink, J.; Bethell, D.; Schiffrin, D. J.; Kiely, C. *J. Chem. Soc., Chem. Commun.* **1995**, 1655–1656.

(3) Hostetler, M. J.; Wingate, J. E.; Zhong, C.-Z.; Harris, J. E.; Vachet, R. W.; Clark, M. R.; Londono, J. D.; Green, S. J.; Stokes, J. J.; Wignall, G. D.; Glish, G. L.; Porter, M. D.; Evans, N. D.; Murray, R. W. *Langmuir* **1998**, *14*, 17–30.

(4) (a) Templeton, A. C.; Hostetler, M. J.; Kraft, C. T.; Murray, R. W. *J. Am. Chem. Soc.* **1998**, *120*, 1906–1911. (b) Templeton, A. C.; Hostetler, M. J.; Warmoth, E. K.; Chen, S.; Hartshorn, C. M.; Krishnamurthy, V. M.; Forbes, M. D. E.; Murray, R. W. *J. Am. Chem. Soc.* **1998**, *120*, 4845–4849. (c) Hostetler, M. J.; Green, S. J.; Stokes, J. J.; Murray, R. W. *J. Am. Chem. Soc.* **1996**, *118*, 4212–4213. (d) Ingram, R. S.; Hostetler, M. J.; Murray, R. W. *J. Am. Chem. Soc.* **1997**, *119*, 9175–9178. (e) Hostetler, M. J.; Templeton, A. C.; Murray, R. W. *Langmuir* **1999**, *15*, 3782–3789.

(5) Leff, D. V.; O'Hara, P. C.; Heath, J. R.; Gelbart, W. M. *J. Phys. Chem.* **1996**, *99*, 7036–7041.

(6) (a) Whetten, R. L.; Khoury, J. T.; Alvarez, M. M.; Murthy, S.; Vezmar, I.; Wang, Z. L.; Stephen, P. W.; Cleveland, C. L.; Luedtke, W. D.; Landman, U. *Adv. Mater.* **1996**, *5*, 428–433. (b) Schaaff, T. G.; Shafiqullin, M. N.; Khoury, J. T.; Vezmar, I.; Whetten, R. L.; Cullen, W.; First, P. N.; Gutierrez-Wing, C.; Ascensio, J.; Jose-Yacamán, M. J. *J. Phys. Chem. B* **1997**, *101*, 7885–7891. (c) Alvarez, M. M.; Khoury, J. T.; Schaaff, T. G.; Shafiqullin, M.; Vezmar, I.; Whetten, R. L. *Chem. Phys. Lett.* **1997**, *266*, 91–98. (d) Schaaff, T. G.; Whetten, R. L. *J. Phys. Chem. B* **1999**, *103*, 9394–9396.

electron microscopy (TEM) and the unique electrochemical QDL charging response of MPC solutions. Theoretical simulations predict that the voltage spacing between MPC QDL charging peaks should respond to changes in MPC core size and dispersity,<sup>7c</sup> and we inspect this here as a tool to follow MPC cluster growth. The combined TEM and double layer charging results show consistent evolutionary features in terms of nanoparticle core size and cluster double layer capacitance ( $C_{\text{CLU}}$ ) as a function of cluster growth time.

### Experimental Section

**Chemicals.**  $\text{HAuCl}_4 \cdot x\text{H}_2\text{O}$  was prepared according to the literature.<sup>8</sup> 1-Hexanethiol (98%, Aldrich), toluene (Mallinckrodt), tetraoctylammonium bromide (98%, Aldrich), tetrahexylammonium perchlorate (99.9%, Fluka), acetonitrile (Fisher), and absolute ethanol (AAPER) were used as received, without further purification. Water was purified by passing house-distilled water through a Barnstead Nanopure system (> 18 M $\Omega$ ).

**MPC Synthesis.** Hexanethiolate MPCs (C6 MPCs) were synthesized according to a literature procedure known to produce Au clusters with an average core of 145 atoms (1.6 nm diameter) covered with 48–50 protecting hexanethiolate chains.<sup>3</sup> Specifically, a toluene solution containing a 3:1 ratio of hexanethiol to  $\text{AuCl}_4^-$  (the gold complex was transferred from the aqueous phase by tetraoctylammonium bromide) was cooled to 0 °C followed by addition of aqueous  $\text{BH}_4^-$  reductant; the deep red toluene layer immediately turned black, indicating MPC formation. The reaction was run on a scale such that ca. 15–20 mL samples of the MPC toluene solution could be removed from the reaction solution at selected time intervals. Cluster growth in these samples was quenched by addition of a 10-fold volume excess of absolute ethanol (precipitating the MPC product; precipitation was complete in ca. 3–5 min). Each precipitated MPC product was isolated by filtering and washed with copious amounts of absolute ethanol, followed by ca. 150 mL of acetone. The MPCs prepared in the above manner were clean of unreacted thiol and of dihexanedisulfide by  $^1\text{H}$  NMR spectroscopy.

**TEM.** TEM samples were prepared by casting a single drop of a  $\sim 1$  mg/mL cluster solution in hexane onto standard carbon-coated (200–300 Å) Formvar films on copper grids (200 mesh) and drying in air for at least 45 min. Phase-contrast images of the particles were obtained with a side-entry Phillips CM12 electron microscope operating at 120 keV. Three typical regions of each sample were obtained at either 430K or 580K magnification. Size distribution histograms of the Au cores were obtained from at least two digitized photographic enlargements using Scion Image Beta Release 2 (www.scioncorp.com).

**Electrochemical Measurements.** Electrochemical measurements were performed using a BAS 100B/W electrochemical workstation. The 0.06 cm<sup>2</sup> Pt disk working electrode was polished prior to each experiment with 0.5  $\mu\text{m}$  diamond paste (Buehler) followed by rinsing with water, ethanol, and acetone. Pt coil counter and Ag quasi-reference (AgQRE) electrodes resided in the same cell compartment as the working electrode. The electrochemical solvent was a 2:1 toluene/ $\text{CH}_3\text{CN}$  (v/v) mixture containing ca. 0.1 mM hexanethiolate MPC and 0.05 M tetrahexylammonium perchlorate as the supporting electrolyte.

### Results and Discussion

**TEM.** TEM has provided important size and shape information about alkanethiolate monolayer-protected

gold clusters. Whetten and co-workers<sup>6a</sup> combined high-resolution TEM with laser desorption/ionization (LDI) mass spectrometry and theoretical modeling studies to predict a truncated octahedral morphology as the equilibrium core shape for alkanethiolate MPCs. Interestingly, the number of core Au atoms in closed-shell truncated octahedral MPC structures tends toward certain stable populations or “magic numbers”, including clusters with 225, 314, and 459 core Au atoms.<sup>6c</sup> Such observations are consistent with assuming an equilibrium core structure model for MPC reaction products, as we have done in our own work.<sup>3</sup> Several TEM studies have illustrated patterned self-assembly in cast MPC films, including characteristic core–core spacings that correlate with some form of interdigitation of chains or chain bundles of the protecting alkanethiolate monolayers.<sup>3,9</sup>

Obtaining core size dispersity information for MPC preparations is also important. TEM histograms of MPC samples often display multimodal distributions with maxima generally repeated in replicate histograms and indicate, in accord with previous work,<sup>3,7</sup> a preference for cluster magic numbers. Previous MPC synthesis studies have focused on the MPC reaction products of a fixed reaction time (typically 12–24 h). Whetten and co-workers, however, report that quenching the reaction at short times (< 15 min) produces larger abundances of MPCs with very small core sizes (< 1.6 nm average diameter).<sup>7a,c</sup>

Figure 1 shows representative TEM images and core diameter histograms (insets, note that the distance scales are not all the same) of hexanethiolate-coated MPCs isolated from a reaction mixture after 0.5, 50, and 125 h reaction times. After 0.5 h (Figure 1a histogram), two population ranges of cluster size appear to have formed: one with number-average core diameter  $1.4 \pm 0.4$  nm (comprises  $\sim 65\%$  of the total MPC population) and another with average core diameter  $2.3 \pm 0.3$  nm (comprises  $\sim 35\%$  of the total MPC population). The overall average core diameter is  $2.0 \pm 1.1$  nm. The population of nanoparticles with average diameters > 3 nm is quite small, in relative terms; these specimens are prominent in the TEM images because of size not population. The above modality is less evident after 50 h of reaction (Figure 1b histogram; the average core diameter has increased to  $2.6 \pm 0.80$  nm) but is slightly more evident after 125 h (Figure 1c histogram), where the population of  $2.0 \pm 1.0$  nm includes  $\sim 55\%$  of the MPCs. The overall average nanoparticle diameter has increased to  $3.1 \pm 1.4$  nm.

The time course of the average core diameter (and variance) in the reaction mixture is shown in Figure 2. The fluctuation in average size at 22 h is probably an artifact. While the variance is substantial, it appears that the average size increases over the course of reaction time. The trend of gradually increasing average core diameter is consistent with the shorter time information of Whetten et al.<sup>7c</sup> Figure 3 gives data for the time course of different core size populations of MPCs. The oscillations in the diameters over short periods of time may or may not be significant, but the trends in the data over longer periods of time are clear. Figure 3a shows that the population of smaller MPCs (diameters < 1.5 nm) drops rapidly during the first few hours of the reaction and then roughly levels

(7) (a) Chen, S.; Ingram, R. S.; Hostetler, M. J.; Pietron, J. J.; Murray, R. W.; Schaaff, T. G.; Khoury, J. T.; Alvarez, M. M.; Whetten, R. L. *Science* **1998**, *280*, 2098–2101. (b) Ingram, R. S.; Hostetler, M. J.; Murray, R. W.; Schaaff, T. G.; Khoury, J. T.; Whetten, R. L.; Bigioni, T. P.; Guthrie, D. K.; First, P. N. *J. Am. Chem. Soc.* **1997**, *119*, 9279–9280. (c) Chen, S.; Murray, R. W.; Feldberg, S. W. *J. Phys. Chem. B* **1998**, *102*, 9898–9907. (d) Hicks, J. F.; Templeton, A. C.; Chen, S.; Sheran, K. M.; Jasti, R.; Murray, R. W.; Debord, J.; Schaaff, T. G.; Whetten, R. L. *Anal. Chem.* **1999**, *71*, 3703–3711. (e) Pietron, J. J.; Hicks, J. F.; Murray, R. W. *J. Am. Chem. Soc.* **1999**, *121*, 5565–5570.

(8) (a) *Handbook of Preparative Inorganic Chemistry*; Brauer, G., Ed.; Academic Press: New York, 1965; p 1054. (b) Block, B. P. *Inorg. Synth.* **1953**, *4*, 14.

(9) (a) Brust, M.; Bethell, D.; Schiffrin, D. J.; Kietly, C. J. *Adv. Mater.* **1995**, *7*, 795–797. (b) Harfenist, S. A.; Wang, Z. L.; Alvarez, M. M.; Vezmar, I.; Whetten, R. L. *J. Phys. Chem.* **1996**, *100*, 13904–13910. (c) Wang, Z. L.; Harfenist, S. A.; Whetten, R. L.; Bentley, J.; Evans, N. D. *J. Phys. Chem. B* **1998**, *102*, 3068–3072. (d) Brust, M.; Kiely, C. J.; Bethell, D.; Schiffrin, D. J. *J. Am. Chem. Soc.* **1998**, *120*, 12367–12368. (e) Fink, J.; Kiely, C. J.; Bethell, D.; Schiffrin, D. J. *Chem. Mater.* **1998**, *10*, 922–926. (f) Baum, T.; Bethell, D.; Brust, M.; Schiffrin, D. J. *Langmuir* **1999**, *15*, 866–871.

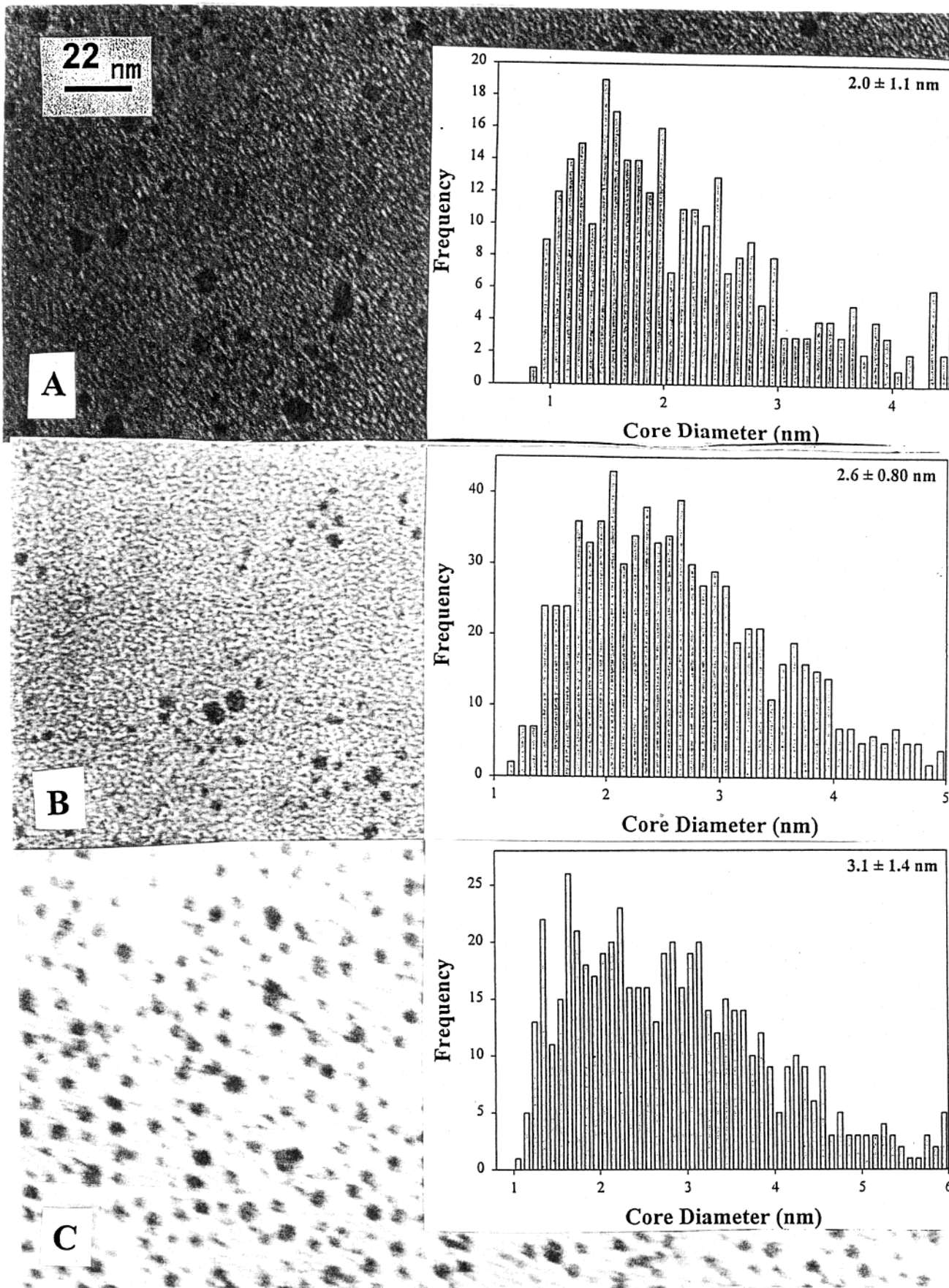


**Figure 1.** TEM and core size histograms (insets) of hexanethiolate MPCs at various reaction times: (A) 0.5 h, (B) 50.5 h, and (C) 125 h. The number-average diameters and standard deviations (variances) for the histograms are noted in the insets.

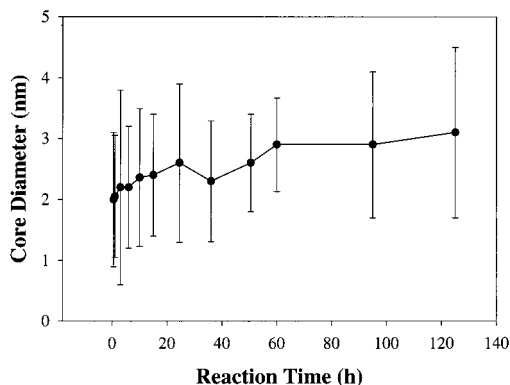


**Figure 2.** Plot of average hexanethiolate MPC core diameter (●) and diameter variance (error bars) as a function of reaction time, as determined from TEM core size histograms from all collected data.

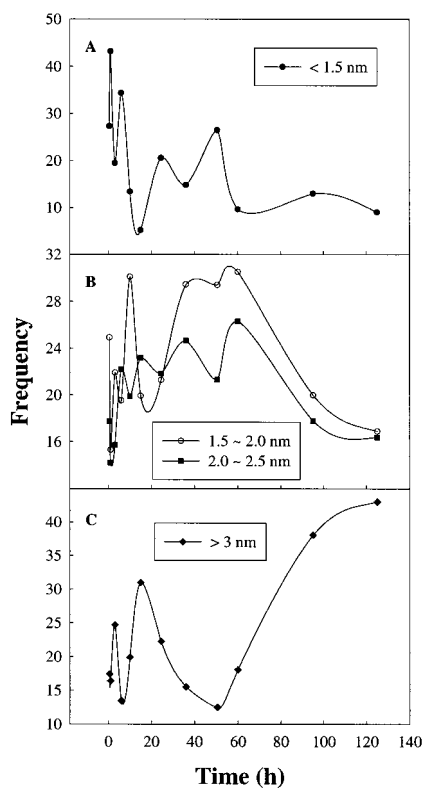


**Figure 3.** Change in MPC core diameter fractional population as a function of time: (A)  $d < 1.5$  nm, (B)  $1.5 < d < 2.0$  nm and  $2.0 < d < 2.5$  nm, and (C)  $d > 3.0$  nm. Lines are in place for eye-guiding only; fluctuations over short time periods are probably not significant.

off, while the population of the larger MPCs climbs steadily after about 50 h (Figure 3c). The populations of intermediate-sized MPCs correspondingly go through a maximum at intermediate times (Figure 3b). (MPCs in the 2.5–3.0 nm range (not shown) account for a relatively small (~10–20%), modestly varying population over the entire time span.)

A nucleation–growth–passivation reaction process is anticipated given the nature of reactions (1) and (2). The TEM results are consistent with this simple picture at relatively short reaction times (<ca. 20 h), but the longer time overall core size increase suggests that further processes that alter core sizes are at work after the initial passivation stage. Some kind of annealing process reduces the population of smaller core MPCs and increases the population of larger ones. The process(es) operates in a

raw and rather complex reaction medium, which contains reactant debris that includes chloride, bromide, and tetraalkylammonium ions, excess thiol, disulfide, and borohydride reagent products. Toluene solutions of isolated, purified MPCs are, in contrast, typically stable in core size for more extended periods (> month), so a certain number of these non-MPC debris species must trigger the growth events in Figures 2 and 3. The complexity of the possibilities makes speculation on detailed chemical mechanisms unwarranted. It also is not possible to distinguish between processes that move single or small numbers of Au moieties from shrinking to growing clusters<sup>10</sup> and processes in which smaller cores fuse to form larger ones; the changes from small to large average core diameters can be accommodated, according to numbers of core atoms, by core fusion. For example, 1.4, 2.0, and 3.0 nm diameter truncated octahedral MPC cores would contain ca. 116, 314, and 976 Au atoms.<sup>3</sup> The data in Figures 2 and 3 thus represent a first but incomplete step in the dissection of reactions (1) and (2). Recent data by Whetten and co-workers<sup>6d</sup> make it clear that etching does occur, but the detailed chemical mechanism of such processes also remains unknown.

**QDL Capacitance Measurements.** The double layer capacitance of MPCs dissolved in electrolyte solutions is sensitive to both the thickness of the monolayer dielectric<sup>7d</sup> and the diameter of the conducting MPC core.<sup>7a,c</sup> This charging is a novel aspect of MPC electrochemistry, because for sufficiently small MPC core sizes it occurs as a single electron or QDL charging event that is observable in room-temperature MPC solutions of uniform core size by a variety of voltammetric procedures.<sup>7</sup> The effect is rooted in the tiny (sub-attoFarad, aF) capacitance ( $C_{CLU}$ ) of the MPC in an electrolyte solution, which causes the voltage increment ( $V$ ) from single electron/MPC events to be  $> k_B T$ , producing well-resolved current peaks in experiments such as those in the differential pulse voltammogram (DPV) of Figure 4.

Although an electrostatically based process, the thermodynamics of one electron QDL charging events have been shown<sup>7c</sup> to formally resemble that of conventional redox reactions (such as the oxidation of ferrocene), including a “formal potential” characteristic of each change-of-core-charge charging event, which referenced to the potential of zero core charge ( $E_{PZC}$ ) is

$$E_{z,z-1}^{\circ} = E_{PZC} + \frac{\left(z - \frac{1}{2}\right)e}{C_{CLU}} \quad (3)$$

where  $E_{z,z-1}^{\circ}$  is the formal potential of the  $z(z-1)$  charge state “couple”. In DPV experiments such as that of Figure 4, the value of  $E_{z,z-1}^{\circ}$  is taken as the average of the positive- and negative-going (dc) potential sweeps (averaging out  $iR_{UNC}$ ). The  $z$  value is signed such that  $z > 0$  and  $z < 0$  correspond to core “oxidation” and “reduction”, respectively. Insofar as  $C_{CLU}$  is potential independent, which seems to be so for potentials not far removed from  $E_{PZC}$ ,<sup>7</sup> this relation predicts a linear plot of  $E_{z,z-1}^{\circ}$  vs charge state, with  $C_{CLU}$  determined from its slope.

Intuitively, and according to simulations,<sup>7c</sup> one expects that QDL peaks will be unresolved and absent in the DPV of solutions of MPCs containing a continuum mixture of core sizes (and thus of  $\Delta V$  values). Previous QDL charging experiments<sup>7a-c</sup> were accordingly conducted on samples of MPCs that had been solubility-fractionated and contained reasonably monodisperse core sizes. We have,

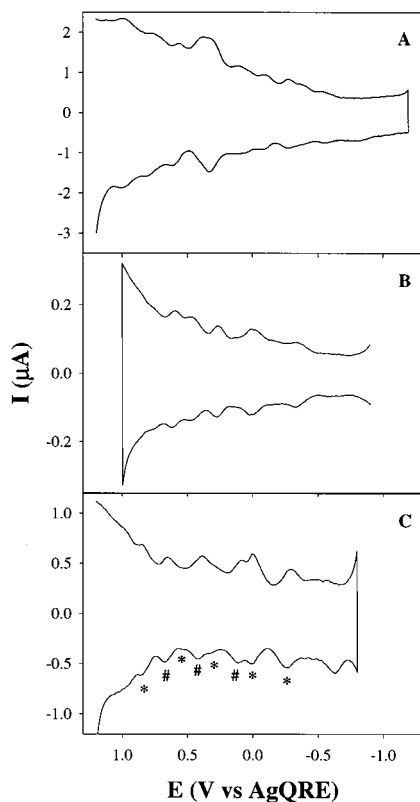


**Figure 4.** Differential pulse voltammograms of ca. 0.1 mM hexanethiolate MPC in 2:1 toluene/CH<sub>3</sub>CN (v/v) at various reaction times: (A) 0.5 h, (B) 50.5 h, and (C) 125 h. Peaks separated by ~0.3 V are denoted with \* in part C while those which have ~0.23 V separation are denoted with #. A dc potential ramp of 10 mV/s and either a 20 (A, B) or 50 mV (C) pulse amplitude were employed. All measurements were acquired on a 0.06 cm<sup>2</sup> Pt working electrode in the presence of 0.05 M THAP supporting electrolyte.

however, recently discovered that QDL charging peaks are also seen in solutions of crude, unfractionated MPCs, most particularly those with hexanethiolate<sup>7d</sup> or arylthiolate<sup>11</sup> monolayers. The DPV traces in Figure 4 are for *unfractionated* MPC samples removed from the MPC synthetic reaction (like those used in the TEM experiments above). Despite the core size dispersity obvious in the Figure 2 histograms, QDL charging peaks are quite discernible at all times, especially at potentials close to  $E_{PZC}$ . Our understanding of DPV quantized charging observations such as Figure 4 is that certain, discrete core size populations must be sufficiently numerous to yield definable charging peaks resting upon a charging current background due to overlapping peaks of other more uniformly populated core (i.e., not very different) sizes. An analysis of core size from the potentials at which the QDL charging peaks appear is therefore a determination selective to these particular populations, as opposed to the *general* determination of core size that results from TEM measurements as in Figures 1–3.

Estimation of the potentials of the QDL peaks in Figure 4 (and other DPV results not shown) leads to the eq 3 plots shown in Figure 5a, as a function of reaction time. The slopes of these plots can be used to evaluate cluster capacitance ( $C_{CLU}$ ) as a function of reaction time, as shown in Figure 5b. There is some obvious uncertainty associated with the fact that more than one prevalent core size cluster population seems to contribute to the DPV peaks; an attempt was made to select from the most regularly spaced

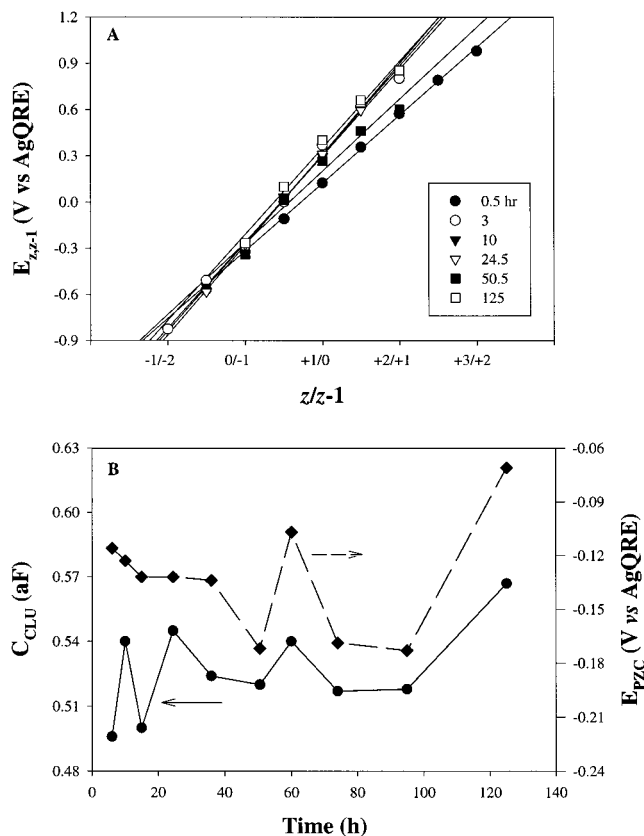


**Figure 5.** (A) Plots of QDL charging peak potentials ( $E_{z,z-1}$ ) vs MPC charge state ( $z$ ) as a function of MPC reaction time, as determined from differential pulse voltammograms from all collected data. Straight lines are the corresponding linear regressions. (B) Variations of MPC potential-of-zero charge ( $E_{PZC}$ ,  $\blacklozenge$ ) and capacitance ( $C_{CLU}$ ,  $\bullet$ ) with reaction times. Lines are for eye-guiding only.

peaks from Figure 4 for the Figure 5a plots. In general, MPC capacitance ( $\bullet$ ) starts out lower (0.49 aF) and, with some fluctuation, levels out (~0.52 aF) before rising at the end of the reaction course (125 h) to 0.57 aF. This trend in  $C_{CLU}$  indicates an increase in the prevalent core size producing the QDL peaks, a result qualitatively consistent with the TEM results presented above.

(The minimum in DPV currents nearest  $-0.2$  V was selected as the potential of zero MPC core charge, following results from an ac impedance study of surface-attached MPCs.<sup>12</sup> The time variation of the actual value of the minimum potential is shown in Figure 5b ( $\blacklozenge$ ); the apparent  $E_{PZC}$  value seems to drift toward more negative values during the reaction but shows a positive jump at the end. The meaning of this change is unclear and may be influenced by the changing  $E_{PZC}$  of the background of closely spaced cluster core sizes.)

Recent studies of the monolayer chain-length dependence of  $C_{CLU}$  of carefully fractionated MPC samples have shown that  $C_{CLU}$  varies with the thickness of the monolayer dielectric in remarkable agreement with a simple concentric sphere capacitance model:<sup>7d</sup>

$$C_{CLU} = 4\pi\epsilon_0\epsilon(r/d)(r + d) \quad (4)$$

where  $\epsilon_0$  is the permittivity of free space,  $\epsilon$  the dielectric constant of the monolayer,  $r$  the MPC core radius, and  $d$  the monolayer dielectric thickness. A value of  $\epsilon = 3$  fits

(11) Chen, S.; Murray, R. W. *Langmuir* **1999**, *15*, 682–689.

(12) Chen, S.; Murray, R. W. *J. Phys. Chem. B* **1999**, *103*, 9996–10000.

the chain-length variation. Given the success of this simple model, eq 4 can be employed to estimate, from an experimental value of  $C_{\text{CLU}}$  and known monolayer chain length, the value of core radius producing that  $C_{\text{CLU}}$  value. Thus, values of  $C_{\text{CLU}} = 0.49, 0.52,$  and  $0.57$  (for the intermediate and extremes of reaction time in Figure 5b) predict not-very-different core diameters of 1.50, 1.56, and 1.66 nm. The core diameter at the intermediate times, assuming a truncated octahedral core shape,<sup>6</sup> corresponds to 145 atoms/Au core, which is the average product of fractionated clusters whose synthesis had been allowed to proceed for 24 h. A fractionated 145 atom MPC has 48–50 hexanethiolate chains and gives a  $C_{\text{CLU}} = 0.53$  aF.<sup>7d</sup>

At the longest reaction time, the DPV result (Figure 4c) is sufficiently well-resolved that a second population (#) of charging peaks, with a smaller  $\Delta V \cong 0.23$  V (giving  $C_{\text{CLU}} = 0.68$  aF), can be resolved from the Au<sub>145</sub> peak spacing (\*) dominant during most of the reaction,  $\Delta V \cong 0.30$  V (giving  $C_{\text{CLU}} = 0.53$  aF). Equation 4 predicts a core diameter of 1.86 nm based on this additional population, which corresponds to cores containing  $\sim 201$  Au atoms. Both of these core sizes are accommodated within the TEM analysis of Figure 1. It should be emphasized that the DPV results do not, apparently because of too closely spaced core sizes, yield information about the broader spectrum of core sizes evident in the TEM images and their analysis.

This research is an important first step in understanding how MPC core size evolves in the Schiffrin cluster synthetic reaction. An understanding of the MPC synthesis reaction will be helpful in eventually designing reactions that

produce smaller and/or more monodisperse core size clusters. We have found that, while the standard TEM method for examining core and dispersity in MPC and other nanoparticle samples is effective, electrochemically based double layer charging can probe narrow-size-range populations that are natural outcomes of a particular reaction mixture. Further information on the core size dependence of QDL charging measurements would further define the utility of this approach. Because the average core size diameter gradually increases over the first 60 h of reaction and then remains largely unchanged afterward (out to 125 h) at  $\sim 3.0$  nm, the results confirm that MPCs of the smallest core size are best obtained by quenching the reaction at relatively early times.<sup>6a-d</sup> The results further suggest that, if one or more of the reaction debris species (see above) is an active participant in core diameter growth, then the smallest core size may also be reached by eliminating such elements from the reaction scheme.

**Acknowledgment.** This research was supported in part by grants from the National Science Foundation (NSF) and Office of Naval Research (ONR). The authors thank Dr. M. J. Hostetler for assistance with TEM measurements. A.C.T. acknowledges support from an Edward G. Weston Electrochemical Society Summer Fellowship and an ACS Division of Analytical Chemistry Graduate Research Fellowship, sponsored by Perkin-Elmer.

LA991206K